

Distribution of continuous heterogeneities in the blocks of optical materials.

Results of interference measurements

W. KOWALIK

Institute of Physics, Technical University of Wrocław, Wybrzeże Wyspiańskiego 27, 50–370 Wrocław, Poland.

Results of measurements of the refractive index distribution in blocks of optical materials (optical glass, neodymium glass, fused quartz, silicon) have been presented. An interference measurement method is described. The measurement accuracies of the method may be as high as 1.10^{-7} for the samples of 1 cm thickness.

1. Introduction

Glass is an amorphous body obtained by overcooling a fused mass, independent of chemical composition and solidification temperature range. As a result of continuously increasing viscosity it has the mechanical properties of solid body, and the transition process from the liquid state to the glassy one is reversible. The properties of the optical glass (including its refractive index) depend on its chemical composition, on the melting process applied and the further thermal treatment of both the glass mass and the semi-processed products made of it [1], [2].

The homogeneity of glass depends, above all, on all kinds of stress and also on the chemical homogeneity (homogenization). Glass being unstressed is isotropic while it is birefringent when stressed. Thermal stress (of the first kind) appears due to solidification of the external layer at first and next the internal layer of the melted mass [1]–[3]. The stress can be reduced by annealing the glass or cutting it into smaller pieces. The characteristic distribution of stresses appears due to liberation of stress as a consequence of cutting out an element from a great mass of melted glass [3], [4]. Also, the external forces evoke stress in glass [5], [6]. The stress of second kind appears due to two-phase structure of glass. There appear complexes in glass, which are characterized by crystalline structure and have the extension coefficient other than the remainder of glass. This kind of stress may be reduced by applying the suitable stabilization of the glass (relaxation).

As may be seen, there are a number of factors which influence the homogeneity of glass. All technological phases and the whole "history" of glass influence its final homogeneity (*cf.* [7], for example). Together with the change of stress also some other properties of glass may change (*cf.* [8], for example). A good measurement method for the refractive index determination should assure a sufficient accuracy and be universal. The interference methods satisfy these requirements, assuring high

accuracy and being rather universal. The results of the heterogeneity measurements which are presented in this work were obtained using the method described in [9], which makes also possible the measurement of the linear component in the refractive index distribution. The method applied enables us to examine the influence of many factors mentioned above on the heterogeneity of glass, including those related to the technology of optical materials production. Also, the measurement of the due birefringence is possible. The results presented in this work, in spite of their preliminary character, are rather interesting and provide a good indication of the further possibilities offered by the method.

2. Principle of measurement

The measurement is made in a laser interferometer of Twyman–Green type (Fig. 1). Three interferograms are made.

– For two-beam interferometry they are to record (Fig. 2a):

1. Interference between the mirrors M1 and M2 through the block examined.
2. Interference between the mirrors M1 and M2, when there is no glass block in the interferometer.
3. Interference between the block surfaces.

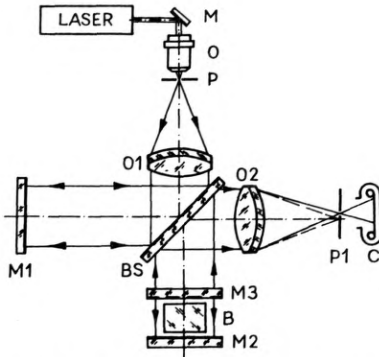


Fig. 1. Laser interferometer of Twyman–Green type. M – directional mirror, OM – microscope objective, P – pinhole diaphragm (spatial filter), O1 – collimator objective, O2 – telescope objective, BM – beam splitter, M1, M2 – interferometer mirrors, M3 – partly transmitting mirror to produce the multipass interference, P1 – diaphragm to select the higher order multipass interference, C – photo or TV camera

– For the multipass interferometry they are to record (MI, Fig. 2b):

1. Interference between the mirrors M1, M2, M3 through the glass block.
2. Interference between the mirrors M1, M2, M3, when there is no glass block in the interferometer.
3. Interference between the block surfaces.

The interferograms 1 and 3 are obtained for the same position of the glass block, while interferograms 1 and 2 are produced for unchanged position of interferometer mirrors, and interferogram 3 is made additionally without the mirrors M1, M2

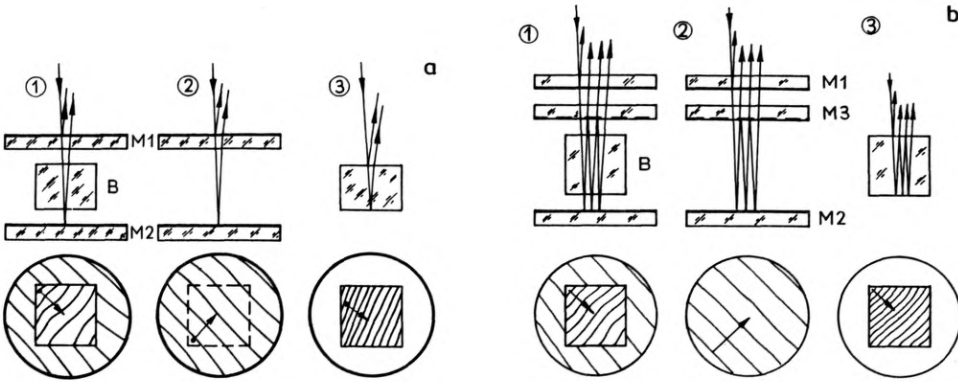


Fig. 2. Three interferograms of the method described. **a** – two-beam interference: 1 – interference between the mirrors M1 and M2 (via the block), 2 – interference between the mirrors M1 and M2 when there is no block in the interferometer, 3 – interference between the surfaces of the glass block examined; **b** – multipass interference: 1 – interference between the mirrors M1, M2 and M3 (via the glass block), 2 – interference between the mirrors M1, M2, M3 when there is no block in the interferometer, 3 – interference between the surfaces of the examined block

or M3. During the preliminary alignment of the mirrors it should be observed on which side of the interferogram the corresponding wedge edge is located. The interference fringes are numbered starting from the side where the wedge is located. At first, it should be established, on which side of the interferogram 3 the due edge is placed. This can be found in the following way. The mirrors of the interferometer should be positioned in a way which increases maximally the interfringe distance for the interferogram 1. The fixing of the wedge edge position (for interferogram 2) between the mirrors M1 and M2 in this case indicates that the wedge edge for the interferogram 3 is located on the opposite side. This follows from the fact that the optical wedge of the glass block has been compensated by the air wedge created between the mirrors M1 and M2. Location of the wedge edge is established according to the known principle (used for the live or dynamic fringes) that while diminishing the interfringe distance the interference fringes move towards the wedge edge.

If δ_x is a difference operator acting along the x axis, then from [9] and Fig. 3 the following magnitudes can be calculated (Tab. 1): difference in the geometric thickness of the glass block $\delta_x L = EF - BC$, difference in the “optical” thickness $\delta_x L_0 = EG - BC$ (where $EGn = EF(n + \delta n)$), difference in the refractive index $\delta_x n$ (which is the difference in the averaged values of the refractive index over the whole thickness of the block L). $L = L' + \delta L$, where L' is the thickness of the block at the reference point. The adjective “optical” which is used here has another meaning than usually. It refers to the geometrical calculations based on optical testing under assumption that $n = \text{const}$. For instance, the optical thickness means the geometrical thickness calculated from the optical measurements under assumption that there exists no refractive index gradient inside the glass block.

All the interferograms present plane interference fields describing the interference under $m = m(x, y)$. Since the analysis of the function of two variables is very

Table 1. Basic measurement formulae derived from analysis of three interferograms

Analysed quantity of	Quantitive to be estimated	Component*	Resultant	
			Modulus	Direction
Interference order	Geometrical thickness difference	$\delta_x L = \frac{\lambda}{2N} (\delta_x m - \delta_x m_b + \delta_x m_0)$	$\delta L = \frac{1}{2} (\delta_x L + \delta_y L)$	
	Optical thickness difference	$\delta_x L_0 = \frac{\lambda}{2nN} \delta_x m_0$	$\delta L_0 = \frac{1}{2} (\delta_x L_0 + \delta_y L_0)$	
	Refractive index difference	$\delta_x n = \frac{n}{L} (\delta_x L_0 - \delta_x L) = \frac{\lambda}{2NL} \times [\delta_x m_0 - n(\delta_x m - \delta_x m_b + \delta_x m_0)]$	$\delta_n = \frac{1}{2} (\delta_x n + \delta_y n)$	
First derivative interference order	Geometrical wedge	$\varphi_x = \partial_x L = \frac{\lambda}{2N} (\partial_x m - \partial_x m_b + \partial_x m_0)$	$\varphi = (\varphi_x^2 + \varphi_y^2)^{1/2}$	$\theta_1 = \arctan \frac{\varphi_y}{\varphi_x}$
	Optical wedge	$\varphi_{0x} = \partial_x L_0 = \frac{\lambda}{2nN} \partial_x m_0$	$\varphi_0 = (\varphi_{0x}^2 + \varphi_{0y}^2)^{1/2}$	$\theta_{10} = \arctan \frac{\varphi_{0y}}{\varphi_{0x}}$
	Refractive index gradient	$\partial_x n = \frac{n}{L} (\varphi_{0x} - \varphi_x) = \frac{\lambda}{2NL} \times [\partial_x m_0 - n(\partial_x m - \partial_x m_b + \partial_x m_0)]$	$\partial n = [(\partial_x n)^2 + (\partial_y n)^2]^{1/2}$	$\theta_{1n} = \arctan \frac{\partial_y n}{\partial_x n}$
Second derivative of interference order	Speed variations of geometrical wedge	$\partial_x \varphi = \partial_x^2 L = \frac{\lambda}{2N} (\partial_x^2 m - \partial_x^2 m_b + \partial_x^2 m_0)$	$\partial \varphi = [(\partial_x \varphi)^2 + (\partial_y \varphi)^2]^{1/2}$	$\theta_2 = \arctan \frac{\partial_y \varphi}{\partial_x \varphi}$
	Speed variations of optical wedge	$\partial_x \varphi_0 = \partial_x^2 L_0 = \frac{\lambda}{2nN} \partial_x^2 m_0$	$\partial \varphi_0 = [(\partial_x \varphi_0)^2 + (\partial_y \varphi_0)^2]^{1/2}$	$\theta_{20} = \arctan \frac{\partial_y \varphi_0}{\partial_x \varphi_0}$
	Speed variations of refractive index gradient	$\partial_x^2 n = \frac{n}{L} (\partial_x \varphi_0 - \partial_x \varphi) = \frac{\lambda}{2NL} \times [\partial_x^2 m_0 - n(\partial_x^2 m - \partial_x^2 m_b + \partial_x^2 m_0)]$	$\partial^2 n = [(\partial_x^2 n)^2 + (\partial_y^2 n)^2]^{1/2}$	$\theta_{2n} = \arctan \frac{\partial_y^2 n}{\partial_x^2 n}$

* X-axis component; for Y-axis, the above formulae are analogue.

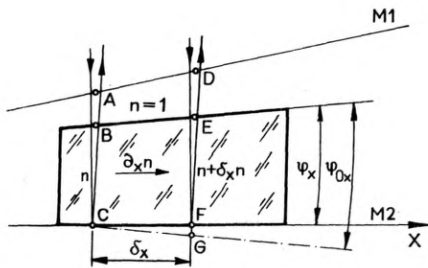


Fig. 3. Influence of grad n on the optical path difference

time-consuming, assume that we are interested only in information at some points, *i.e.* in the sites of the scanning network. The scanning networks should be sufficiently dense to enable a sufficiently accurate description of the character of the measured magnitudes and should be located at the same places on the three interferograms. The analysis of interferograms is carried out along the scanning lines, both vertical and horizontal. Such a procedure renders it possible to replace the function of two variables by functions of single variables the number of which is equal to that of the scanning lines. The scanning of interferograms consists in measuring the coordinates of the fringe centres on the scanning lines and attributing to them the suitable orders of interference, *i.e.* the numbers of fringes. Since such a functional relation is given at certain points only, therefore, to recognize it more accurately, an optimal approximation must be carried out, and for the coordinates of sites the values of the function m must be calculated as well as its first derivative ∂m and the second derivative $\partial^2 m$. Next, basing on both these data and the others concerning the block, all the magnitudes following from the formulae from Tab. 1 are calculated. The whole process is carried out by computer which is fed with the data obtained from the scanning of the three interferograms. Since the interference measurement is relative, a reference point (site) must be chosen with respect to which all the differences of the corresponding magnitudes will be calculated. In the considerations below, the reference point was chosen as the middle point of the sample.

1. Knowing the differences in the interference orders δm , δm_b , δm_0 , the geometric difference of the block thickness $L\delta$, the "optical" thickness differences δL_0 in the block, and the refractive index difference δn are calculated.

2. Knowing the first derivations of the interference order ∂m , ∂m_b , ∂m_0 , the following magnitudes are calculated: geometric wedge φ , "optical" wedge φ_0 and refractive index gradient δn .

3. Knowing the second derivative of the interference orders: $\partial^2 m$, $\partial^2 m_b$, $\partial^2 m_0$, it is calculated how quick the geometric wedge, the "optical" wedge and the gradient of the refractive index ($\partial\varphi$, $\partial\varphi_0$, $\partial^2 n$) are changing.

Since the magnitudes described in points 2 and 3 are vectors, their x and y components and next the resulting vectors are calculated together with the directions θ of their maximal changes (θ is measured in the direction from the positive horizontal coordinate to the positive vertical coordinate in the block).

When applying the multiple interference the distance between the interference fringes amounts to $\lambda/(2N)$, where N is the order of interference (for two-beam interference $N = 1$).

The method of scanning may be also applied in one direction only, *i.e.*, along the scanning line positioned more or less in the direction perpendicular to the interference fringes. When applying the approximation and the suitable programme for computer, it is easy to pass from the coordinates connected with new scanning lines to the coordinates x, y connected with the block and calculate $m = m(x, y)$. This manner is especially useful when the interferograms are not photographed but aerial images are immediately scanned by a special device, for instance, TV CCD camera with the Frame Grabber installed in the PC IBM computer.

3. Results of measurements

The measurements were made for optical glass produced in Jelenia Góra Optical Works (Poland). This is a typical optical glass fabricated without any special requirements. The glass blocks were examined mainly using the two-beam interference technique since the examined heterogeneities were relatively high and this method offered sufficient accuracy. The interferometer was covered with a thermoisolator during measurement and located on an antivibrational table. The maximal differences in temperature inside the interferometer did not exceed 0.05°C in the air, and 0.03°C inside the glass block. The data obtained from the scanning of the interferometer, *i.e.*, the fringe numbers and their coordinates on the scanning lines were introduced to the computer, which calculated all the quantities described earlier (Tab. 1) on the basis of a suitably elaborated programme. The number of scanning network sites, for which the measurement results are obtained, is not limited and for the examined blocks was as high as 25–225. The glass blocks (Tab. 2) were examined repeatedly for different configurations of interferometer mirrors and

Table 2. Sizes of the measured glass blocks

Block number	Glass denotation	Dimensions [cm]		
		X	Y	Z
1	BaK 571 557	5.00	2.50	5.00
2	BK 518 639	4.83	4.81	4.78
3	BK 518 639	2.52	2.51	2.52
4	F 624 361	3.53	3.55	3.59
5	quartz	$\phi = 5.00$		1.93
6	neodymium	2.54	3.02	20.58
7	neodymium	$\phi = 1.98$		15.00
8	neodymium	$\phi = 1.96$		30.40
9	SK 591 610	5.70	5–5.1	14.60
10	Si*	$\phi = 2.81$		0.355
11	SK 615 584	$\phi = 3.0-3.2$		10.02
12	SK 591 610	3.98	4.97	7.90

* Semiconductor, $\lambda = 1152 \text{ nm}$.

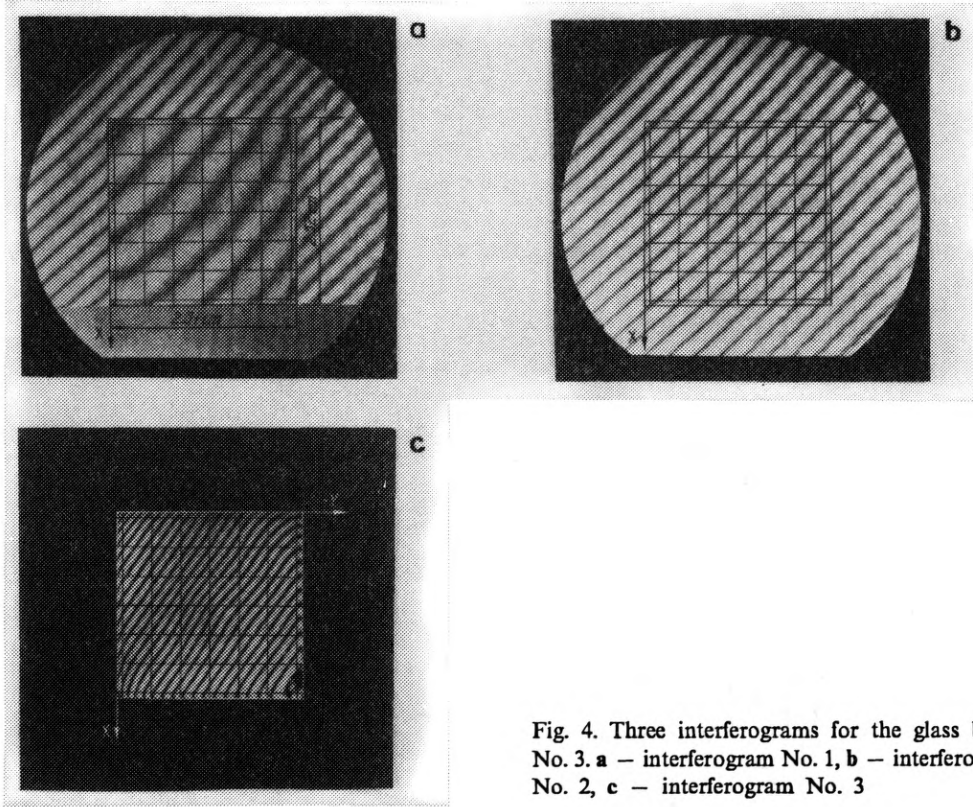


Fig. 4. Three interferograms for the glass block No. 3. **a** – interferogram No. 1, **b** – interferogram No. 2, **c** – interferogram No. 3

for different geometric wedges of the block (its surfaces being polished). This was done in order to determine the error of a single measurement, to recognize the character of the examined changes and to choose the most advantageous method of approximation. It has been found that the method of equalizing the measurement results by applying the approximation increases the accuracy of the measurement $\Delta(\delta n)$ in comparison to the calculated accuracy of a single measurement (Tab. 3) by about 4 times for low measurement accuracies and by about 2 times for higher accuracies. In Fig. 4, interferograms for the block No. 3 are shown, while the results of measurement are shown in Fig. 5. A characteristic feature of these results is the domination of the continuous changes of the linear component of the refractive index. For the same block but for some other directions of testing the nonlinear changes are predominant. The nonlinear character of changes appears also in the glass block No. 9 (Fig. 6) produced in a continuous melting line, with the lateral

Table 3. Calculated measurement errors for some glass blocks

Block number	L [cm]	$\Delta(\delta L)$ [nm]	$\Delta(\delta n)$ [10^{-6}]	$\Delta(\partial n)$ [10^{-6}]
3	2.52	25	2.1	8.6
8	30.40	20	0.14	0.5
9	14.60	24	0.2	0.5
10	0.355	63	7.0	11.0

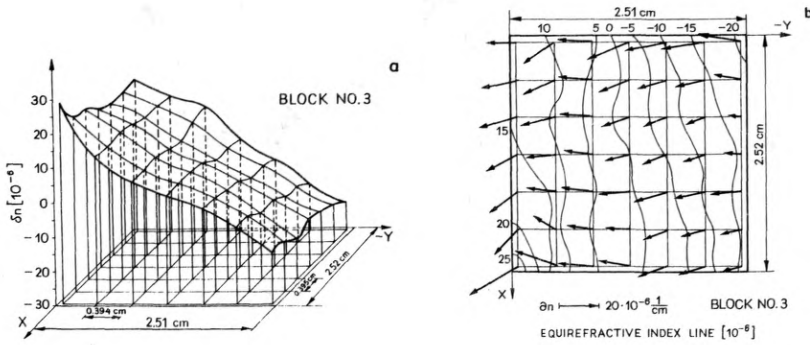


Fig. 5. Changes of the refractive index for the glass block No. 3 (a), and refractive index distribution and its gradients for the glass block No. 3 (b)

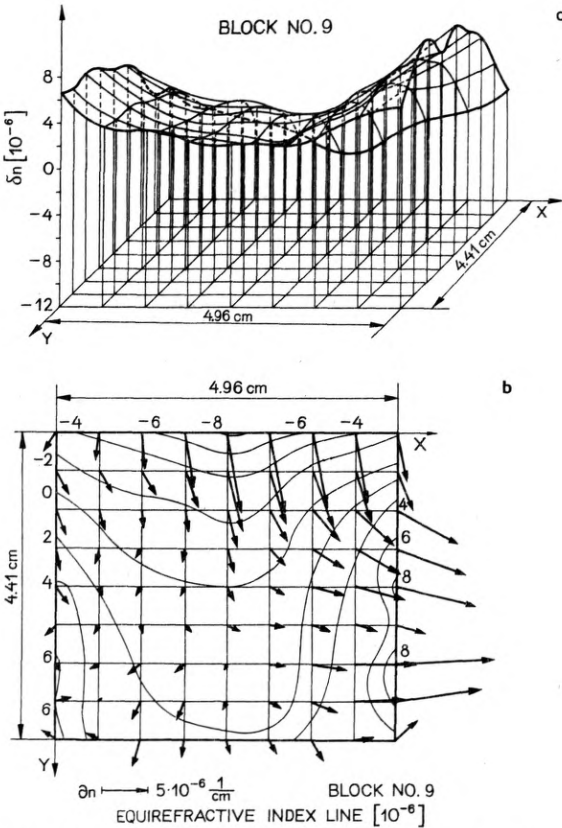


Fig. 6. Changes of the refractive index for the glass block No. 9 (a), and the refractive index distribution and its gradients for the glass block No. 9 (b). (This block was produced in a continuous melting line. The question is if the technological process has been recorded in the refractive index distribution. The technological dimensions of the cross-section of the glass block are 5.7 cm x 5.1 cm. The direction of the gravitational vertical is consistent with the Y axis)

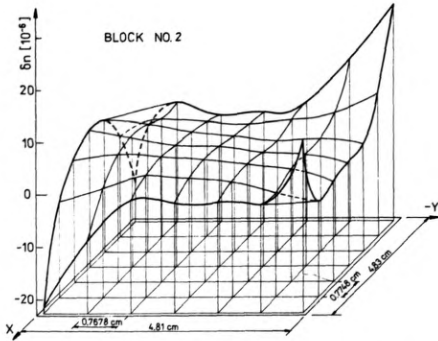
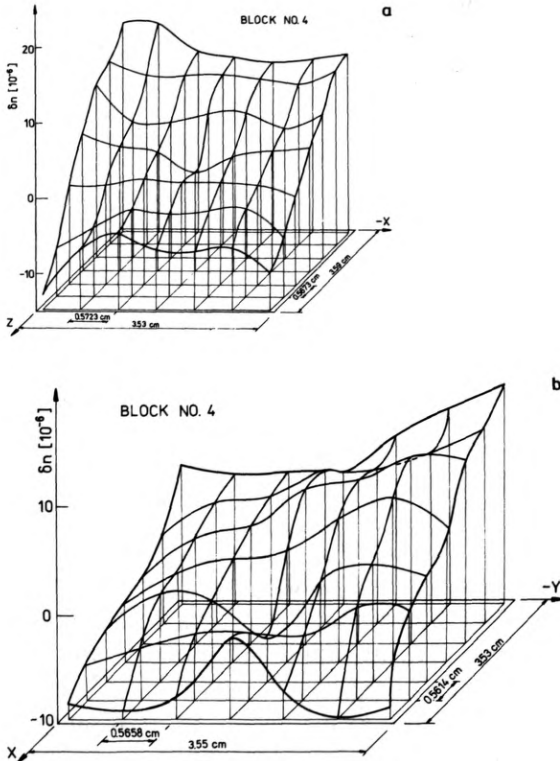


Fig. 7. Refractive index distribution in the glass block No. 2

sides of the block being not processed. Does this mean that some technological process has been recorded, as it is suggested by a characteristic distribution of the refractive index? For the block No. 2 (Fig. 7) in its central part the refractive index does not change almost at all. Some rather significant nonlinear changes are observed in the vicinity of the edges. In Figure 8, the results for the block No. 4 are presented for three surveying directions. In Figure 8a, the linear component



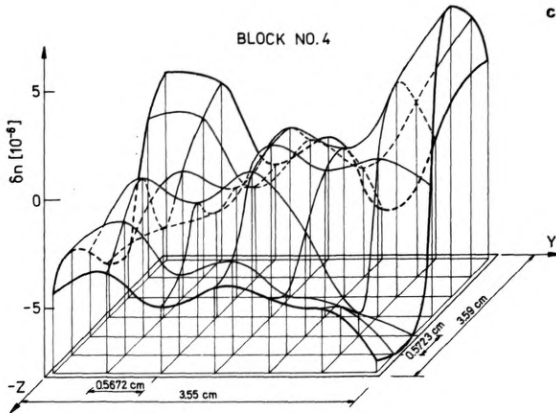


Fig. 8. Refractive index distribution in the glass block No. 4: a – Y-surveying direction, b – Z-surveying direction, c – X-surveying direction

is predominant. In Figure 8b, the linear component is less but the nonlinear components are slightly greater. In Figure 8c, the nonlinear components are predominant but their maximal changes are less than the changes in Fig. 8a and Fig. 8b. Thus, by choosing the suitable surveying direction (and the suitable direction of cutting out the elements from the block), the influence of the heterogeneities on the worsening of the imaging quality may be diminished.

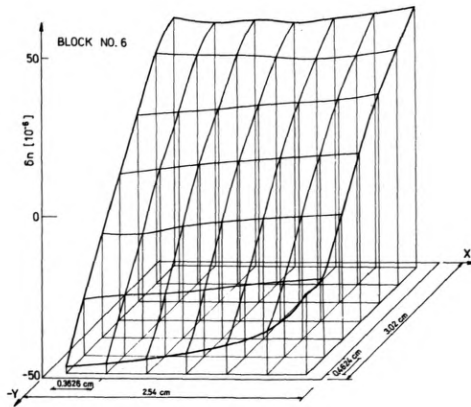


Fig. 9. Refractive index distribution in a bar of neodymium glass of JZO (Poland) production (glass block No. 6)

In Figure 10, the measurement results for the disc made of the melted quartz are presented. Here the spherical changes are predominant. The linear component is also visible. In Figures 9, 11 and 12, the results of neodymium bar examination (used to laser production at the Technical Military Academy, Warsaw) are shown. For one of the first bars produced in Jelenia Góra Optical Works the measurement results are shown in Fig. 9. The linear changes are predominant. They are rather great, hence

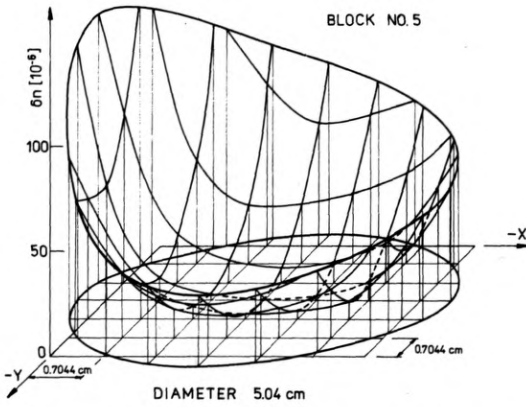


Fig. 10. Refractive index distribution in a disk of melted quartz (glass block No. 5)

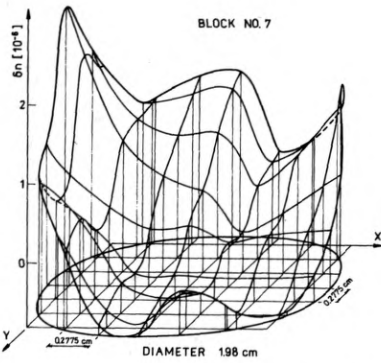


Fig. 11. Refractive index distribution in a bar of neodymium glass of former GDR production (glass block No. 7)

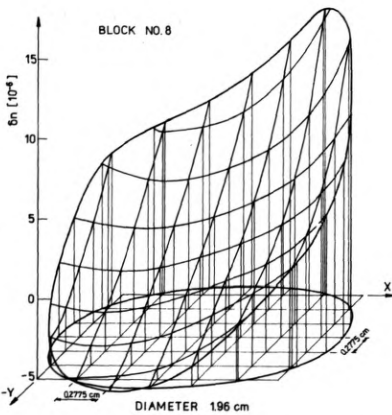


Fig. 12. Refractive index distribution in a bar of neodymium glass of former GDR production (glass block No. 8)

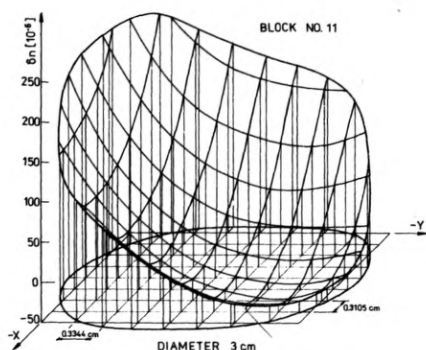
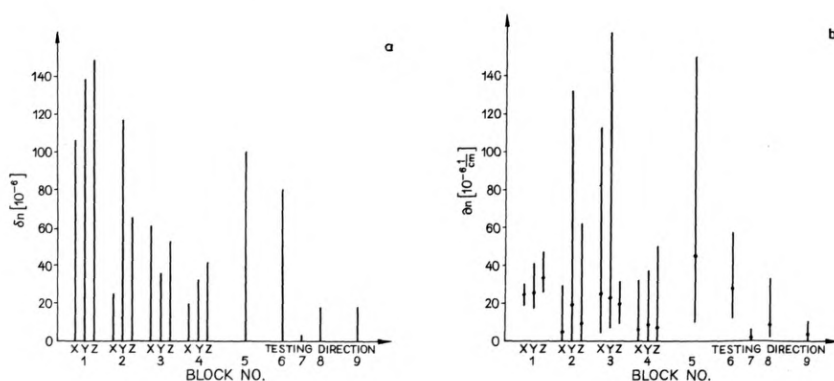


Fig. 13. Refractive index distribution in a bar produced in a continuous melting line (the glass block No. 11). The technological diameter of the bar is 3.0–3.2 cm. The direction of the gravitational vertical is from the block centre to the intersection point of X and Y axes

the nonlinear factor is poorly visible. Our remarks concerning the technological changes allowed us to diminish significantly the gradients of the refractive index in the next melts. Very small changes of the refractive index occur in a neodymium bar (produced in the former GDR) of a circular cross-section (Fig. 11). Here, the nonlinear changes are predominant, being rather small. For another bar which is of circular cross-section as well (produced also in GDR) the results of measurements are presented in Fig. 12. Here, the linear changes are predominant. Among the small nonlinear changes the spherical component is predominant. In Figure 13, the results of measurements for a bar produced in a continuous melting line are presented. The lateral sides of the bar remained unprocessed. Here, a big linear component is predominant which is superposed by nonlinear changes. These changes are dominated by the spherical component. In Figure 14, the typical changes of refractive index for some blocks are presented. The ranges of changes are marked, as well as the average values. Such presentation is rather a general one but it gives an idea of the magnitudes of the described nonuniformities in the glass blocks. In Figure 15, the distribution of the refractive index in the block No. 12 is shown, which was produced also in a continuous melting line but its lateral sides were processed. Both the linear and nonlinear components exist.



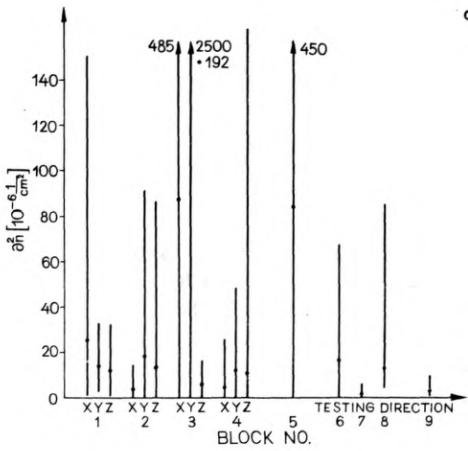


Fig. 14. Ranges of the refractive index differences in glass blocks: a — ranges of the absolute values of refractive index in glass blocks, b — ranges of the absolute values of the gradient refractive index in glass blocks, c — ranges of the refractive index gradient rate change in the blocks

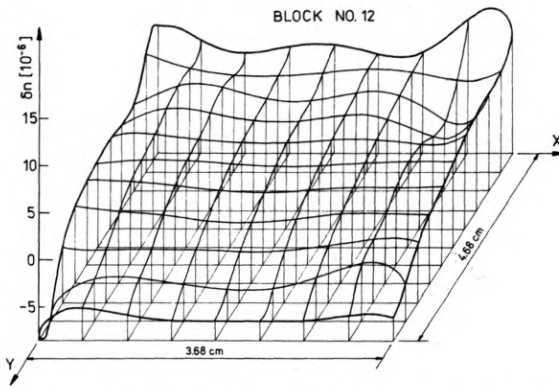


Fig. 15. Refractive index distribution in the glass block No. 12 which was produced in a continuous melting line. Lateral surfaces of the block were processed

In the results presented, the attention was paid to the measurement of the refractive index distribution or their gradients. The present method renders similar measurement possibilities as those described earlier which may be applied to

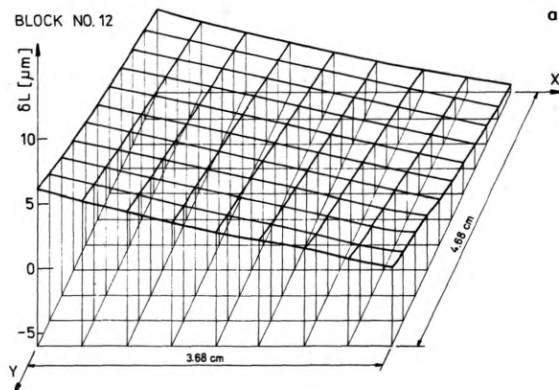


Fig. 16a

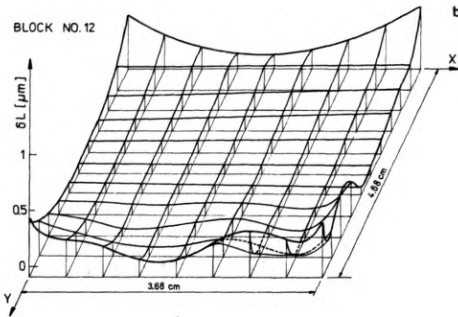


Fig. 16. Thickness distribution in the glass block No. 12. The changes of wedge are predominant (a). Thickness distribution in the same block after a partial compensation of the linear changes (b)

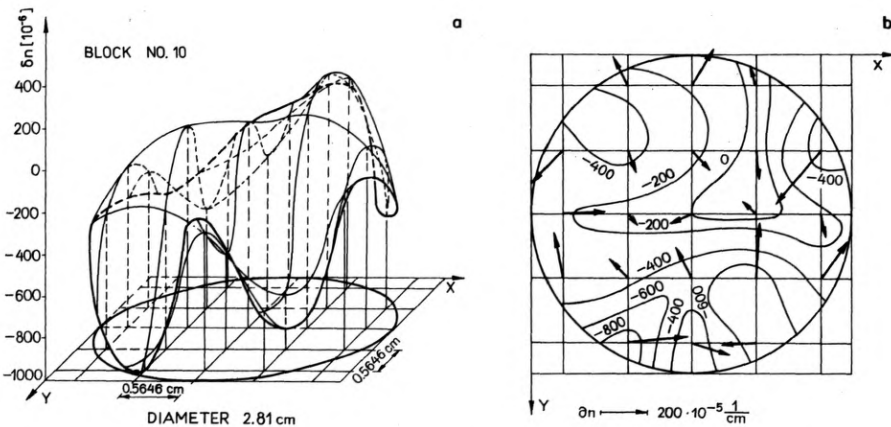


Fig. 17. Measurements of the samples No. 10 of the polycrystalline silicon: a – spatial distribution of the refractive index, b – distributions and gradient of the refractive index

measurement of other magnitudes. For example, in Fig. 16 the results of thickness distribution measurements of the examined block No. 12 are presented. The great linear component (wedge) causes that the nonlinear changes are weakly visible (Fig. 16a). After a partial compensation of the linear changes, the nonlinear changes are better visible in Fig. 16b.

The heterogeneity measurements for phase objects need not be restricted to the visual range. As an example (Fig. 17), the results of the refractive index distribution measurements in a disc (block No. 10) of a polycrystalline silicon are given. The measurements were carried out in infrared light of $\lambda = 1152$ nm, [10].

4. Conclusions

The analysis of the measurement accuracies was given in [9] and in Table 3. The measurement results presented show typical distributions of the refractive index in optical materials and also some investigating possibilities of the method. The

results are of preliminary character as far as the examinations of heterogeneities in optical glasses are concerned in order to improve their production technology. For the last case, the knowledge of the production technology as well as the whole "history" of the optical glass blocks are necessary to come to the proper conclusions. The author does not know such a detailed history of the blocks examined in this work. Only in few of them the direction of the gravitational vertical can be established. Since the results of measurements are influenced by different factors, the individual effects may be examined after having performed some specialized investigations. This should be a series of comparison examinations, with the history of particular samples being known (*i.e.*, the production technology applied, direction of the gravitational vertical, location inside the crucible during the glass transformation and above all the temperature distribution inside the crucible or later inside the annealing chamber). From the present examinations, it follows that the temperature conditions occurring during all the stages of technology have most probably the predominating influence on the homogeneity of the glass and for the samples very well annealed the stresses liberated as a result of cutting out the samples from a greater piece of glass (for instance, spherical components, in the refractive index distribution in the blocks of circular cross-section) are the most decisive. The problems mentioned above as well as the possibility of birefringence measurements using this method will be the subject of the next works.

References

- [1] LEGUN Z., *Technologia elementów optycznych* (in Polish), [Ed.] WNT, Warszawa 1982.
- [2] GOMELSKIJ M. S. *Tonkij otzhig opticheskovo stekla* (in Russian), Mashinostroenie, Leningrad 1969.
- [3] RATAJCZYK F., LISOWSKA B., PIETRASZKIEWICZ K., *Opt. Appl.* 4 (1974), 41.
- [4] ZARÓWNY J., RATAJCZYK F., *Opt. Appl.* 1 (1971), 29.
- [5] REITMAYER F., SCHUSTER E., *Appl. Opt.* 11 (1972), 1107.
- [6] SADEJ J., *Influence of mechanical stresses on changes of refractive index in some optical glasses*, Master's Thesis (in Polish), Institute of Physics, Technical University of Wrocław, Wrocław 1978 (unpublished).
- [7] PAWLIK E., KOWALIK W., *Opt. Appl.* 14 (1984), 177.
- [8] RATAJCZYK F., *Pomiary, Automatyka, Kontrola* (in Polish), No. 11 (1960), 463.
- [9] KOWALIK W., *Appl. Opt.* 17 (1978), 2956.
- [10] KOWALIK W., *SPIE* 136 (1977), 8.

Received January 15, 1993